Berg Huettenmaenn Monatsh (2020) Vol. 165 (3): 125–136
https://doi.org/10.1007/s00501-020-00961-8

BHM Berg- und Hüttenmännische Monatshefte

Production Tools Made by Additive Manufacturing Through Laser-based Powder Bed Fusion

Nader Asnafi[1], Jukka Rajalampi[2], David Aspenberg[3], and Anton Alveflo[4]

[1]School of Science and Technology, Örebro University, Örebro, Sweden
[2]RISE IVF, Olofström, Sweden
[3]DYNAmore Nordic, Linköping, Sweden
[4]voestalpine High Performance Metals, Mölndal, Sweden

Received February 7, 2020; accepted February 8, 2020; published online March 3, 2020

Abstract: This paper deals with the design and production of stamping tools and dies for sheet metal components and injection molds for plastic components. Laser-based Powder Bed Fusion (LPBF) is the additive manufacturing method used in this investigation. Solid and topology optimized stamping tools and dies 3D-printed in DIN 1.2709 (maraging steel) by LPBF are approved/certified for stamping of up to 2-mm thick hot-dip galvanized DP600 (dual-phase steel sheet). The punch in a working station in a progressive die used for stamping of 1-mm thick hot-dip galvanized DP600 is 3D-printed in DIN 1.2709, both with a honeycomb inner structure and after topology optimization, with successful results. 3D printing results in a significant lead time reduction and improved tool material efficiency. The cost of 3D-printed stamping tools and dies is higher than the cost of those made conventionally. The core (inserts) of an injection mold is 3D-printed in DIN 1.2709, conformal cooling optimized and 3D-printed in Uddeholm AM Corrax, and compared with the same core made conventionally. The cooling and cycle time can be improved, if the injection molding core (inserts) is optimized and 3D-printed in Uddeholm AM Corrax. This paper accounts for the results obtained in the above-mentioned investigations.

Keywords: Additive manufacturing, Metal, Powder bed fusion, Stamping, Injection molding, Tools, Design, Topology, Cooling, Optimization

Herstellung von Produktionswerkzeugen mittels additiver Fertigung durch laserbasiertes Pulverbettschmelzen

Zusammenfassung: Dieser Beitrag befasst sich mit dem Deisgn und der Herstellung von Stanzwerkzeugen und Matrizen für Blechkomponenten und Spritzgussformen für Kunststoffkomponenten. Das lasergestützte Pulverbettschmelzen (LPBF) ist das in dieser Untersuchung verwendete additive Fertigungsverfahren. Festkörper und topologieoptimierte Stanzwerkzeuge und Matrizen, die von LPBF aus DIN 1.2709 (martensitaushärtender Stahl) 3D-gedruckt werden, sind für das Stanzen von bis zu 2 mm dickem, feuerverzinktem DP600 (Dualphasen-Stahlblech) zugelassen/zertifiziert. Der Stempel in einer Arbeitsstation in einem Werkzeug zum Stanzen von 1 mm dickem, feuerverzinktem DP600 wird aus DIN 1.2709 3D-gedruckt, sowohl mit einer wabenförmigen Innenstruktur als auch nach einer Topologieoptimierung, mit erfolgreichen Ergebnissen. Der 3D-Druck führt zu einer deutlichen Reduzierung der Vorlaufzeit und einer verbesserten Materialeffizienz des Werkzeugs. Die Kosten für 3D-gedruckte Stanzwerkzeuge und Matrizen sind höher als die Kosten für konventionell hergestellte Werkzeuge. Der Kern (Einsätze) einer Spritzgussform wird aus DIN 1.2709 3D-gedruckt, die konforme Kühlung optimiert und asu Uddeholm AM Corrax 3D-gedruckt und mit dem gleichen, konventionell hergestellten Kern verglichen. Die Kühl- und Zykluszeit kann verbessert werden, wenn der Spritzgießkern (Einlegeteile) aus Uddeholm AM Corrax optimiert und 3D-gedruckt wird. In diesem Beitrag werden die Ergebnisse der oben genannten Untersuchungen dargestellt.

Schlüsselwörter: Additive Manufacturing, Metall, Pulverbettschmelzen, Stanzen, Spritzgießen, Werkzeuge, Design, Topologie, Kühlung, Optimierung

N. Asnafi (✉)
School of Science and Technology,
Örebro University,
SE-701 82 Örebro, Sweden
nader.asnafi@oru.se

1. Introduction

The state-of-the-art for additive manufacturing of metals is described in [1]. Additive manufacturing is subject to a technology assessment in [2]. Based on these and other relevant reviews, the research needs and challenges for the Swedish industrial use of metal additive manufacturing were identified [3]. The development of new metal powders and the use of the new design options were among the identified needs and challenges in [3]. This investigation deals with tool design and production using Additive Manufacturing through Laser-based Powder Bed Fusion (LPBF), henceforth even called AM or 3D-printing. Stamping tools and dies and injection molding core/inserts are the tool types that this study focuses on.

AM of production tools and dies have been studied in different investigations. Tooling for hot sheet metal forming or press hardening was studied in [4]. This investigation showed that AM enables new design approaches for the cooling systems and increased cooling rate in hot sheet metal forming tools. The present investigation will focus on tools and dies for stamping at ambient temperature.

In [5], inserts in a body panel stamping tool were 3D-printed in maraging steel DIN 1.2709. The 3D-printed inserts exhibited the same performance as the conventionally made, however, with reduced lead time and minimized internal process logistics [5]. In the present study, AM is certified industrially and attempts are made to accomplish further improvements by topology optimization of the stamping tools.

AM of tooling in injection molding of plastic components have been studied in different investigations [6, 7]. In [7], optimized conformal cooling enabled by AM replaced the conventional drilled cooling and resulted in shorter cycle time, reduced waste and improved part quality. In this study, the potential of AM is explored both in conventional and simulation-based tool design. This study comprises also testing of a new metal powder for 3D-printing of injection molding cores.

AM of production tools is held to have reached level 8 in manufacturing readiness [8]. This high level is believed to have resulted in a shorter lead time, reasonable costs, and improved functionality. This investigation will evaluate these possibilities.

Concerning the costs, the following two commonly accepted views need to be considered (Figs. 1 and 2):

- The *tool* manufacturing costs: The current AM technology/process results in almost the same unit cost, regardless of the production volume size. The ongoing development of AM is held to result in a reduction of the cost level in the future. Conventional manufacturing yields low costs at large production volumes, while AM is currently held to be beneficial at small production volumes. For tool making where a single or only a few units are made, AM should, therefore, result in lower costs (Fig. 1).
- The *part* manufacturing costs: For parts that require production tooling, the costs of this tooling constitute an initial investment which might be larger for an AM inclusive process. Yet, the total cost per produced part is reduced due to improved cooling and shorter cycle time using production tools made by an AM inclusive process (Fig. 2).

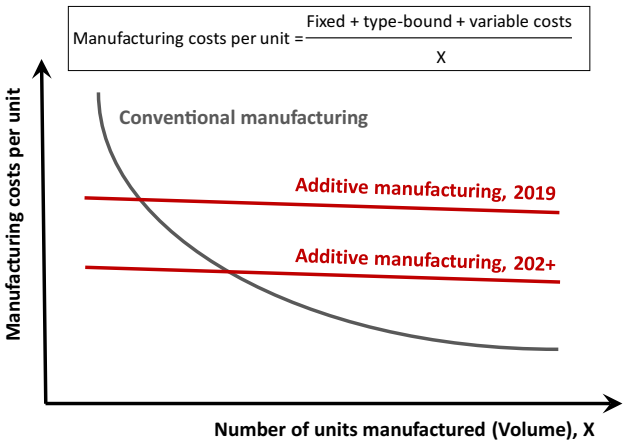

Fig. 1: Conventional and additive manufacturing: manufacturing cost per unit versus the production volume

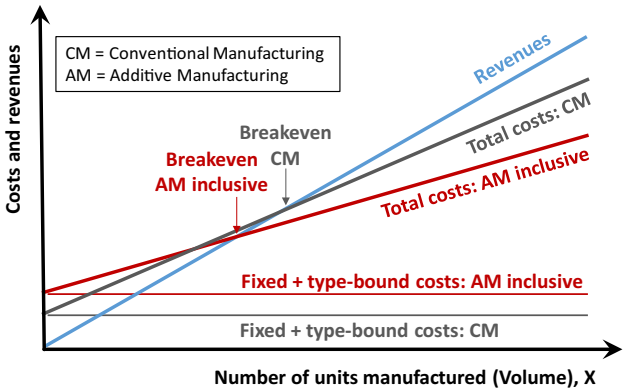

Fig. 2: The costs and revenues: conventional versus AM inclusive fabrication

In this investigation, both of these views are studied and evaluated.

The number of metallic materials that can be used to 3D-print tools, dies and molds is still limited [9]. Among these few existing powder metals, the maraging steel DIN 1.2709 is held to be applicable in tool making for stamping [5]. This investigation focuses on the performance of solid and topology optimized stamping tools and dies 3D-printed in DIN 1.2709. Uddeholm AM Corrax was launched as a powder metal for additive manufacturing of injection molds. The properties of AM Corrax and the performance of an industrial injection mold with conformal cooling channels and 3D printed in this material will be explored in this investigation.

The maximum size that can be 3D-printed by LPBF today is 500 mm × 500 mm × 500 mm [9]. This investigation explores the potential of AM, despite this size limitation.

This paper is an account of the results of the studies mentioned above.

2. Materials

Table 1 displays the chemical composition and Table 2 shows the mechanical properties of maraging steel DIN 1.2709. To determine these properties (Table 2), 5 tensile specimens (circular cross section, φ5 mm) per direction were 3D-printed, heat-treated, machined, and tested. Table 2 displays the average values. 3D Systems ProX DMP and the AM process parameters in Table 7 were used to make these specimens. The heat treatment was conducted at 490 °C in 6 h, after which the specimens were allowed to cool down in the furnace (in air).

A 2-mm thick hot-dip galvanized DP600 was used as the work-piece material in the certification of 3D-printed stamping tools and dies. The chemical composition and properties of this material are shown in Tables 3 and 4 respectively.

Table 5 shows the chemical composition of Uddeholm Corrax. Mechanical properties of the conventional Corrax and AM Corrax, 3D-printed vertically and horizontally are shown in Table 6. To determine these properties (Table 6),

TABLE 1
Chemical composition of maraging steel DIN 1.2709 [10]

Element	Fe	Ni	Co	Mo	Ti	Si	Mn	C
Weight %	Balance	17.0–19.0	9.0–11.0	4.0–6.0	0.9–1.0	≤1.0	≤1.0	≤0.03

TABLE 2
Mechanical properties of maraging steel DIN 1.2709 after AM and heat treatment

	Built vertically	Built horizontally
Yield strength, $R_{p0.2}$ (MPa)	1999	1977
Tensile strength, R_m (MPa)	2120	2167
Hardness (HRC)	56	56

TABLE 3
Chemical composition of the 2-mm thick sheet of DP600 [11]

Element	Fe	P	S	Al	Cr	Si	Mn	C
Weight %	Balance	≤0.02	≤0.004	≥0.020	≤0.50	≤0.30	≤1.66	≤0.120

TABLE 4
Properties of the 2-mm thick sheet of DP600 [11]

Sheet thickness (mm)	2.0
Yield strength, $R_{p0.2}$ (MPa)	350–480
Tensile strength, R_m (MPa)	600–700
Fracture elongation, A_{80} (%)	≥18
Hot-dip galvanized: Layer thickness (μm)/weight (g/m^2)	10 (per side)/140

TABLE 5
Chemical composition of Uddeholm Corrax/AM Corrax

Element	Fe	Ni	Cr	Mo	Al	Si	Mn	C
Weight %	Balance	9.2	12.0	1.4	1.6	0.3	0.3	0.03

TABLE 6
Mechanical properties of Uddeholm Corrax and AM Corrax after ageing

	Conventional Corrax	AM Corrax—built vertically	AM-Corrax—built horizontally
Yield strength, $R_{p0.2}$ (MPa)	1600	1640	1560
Tensile strength, R_m (MPa)	1700	1700	1650
Hardness (HRC)	Up to 50 HRC in aged condition		

TABLE 7
The used 3D printers and AM process parameters

Material (tool material)	Used 3D printer	Layer thickness (μm)	Laser power (W)	Scan speed (mm/s)	Hatch distance (μm)
DIN 1.2709	3D Systems ProX DMP 300	40	185	1200	70
Uddeholm AM Corrax	EOS M290	30	170	1250	100

5 tensile specimens (circular cross section, φ 5 mm) per direction were 3D-printed, solution treated, aged, machined, and tested. Table 6 displays the average values. EOS M290 and the AM process parameters in Table 7 were used to make these specimens. Solution treatment was conducted at 850 °C for 0.5 h (30 min) followed by an aging at 525 °C for 4 h. Ageing can be conducted in the range of 425–600 °C, which creates a microstructure of fine intermetallic precipitates in a martensitic matrix. Hardness is in the range of 34–50 HRC depending on the ageing conditions. The welding behavior is satisfactory and no pre-heating is required.

3. Experimental Procedure

3.1 Stamping Tools and Dies

An experimental procedure is used at Volvo Cars to certify (approve or disapprove) a selected tool concept for stamping of a targeted sheet material grade. This procedure was applied in this investigation. According to this procedure, the selected tool concept (i.e. tool material, hardening method, surface roughness, and coating) is used to make

- a so-called U-bend forming tool. This tool is set up in an eccentric press with a press speed of 60 strokes/minute. The sheet material grade of interest is formed in a U-bend shape with a draw depth of 50 mm in this tool. The binder force is set so that the strain level in the U-bend wall is 60% of FLC_0, the minimum level of the Forming Limit Curve of the selected sheet material. The approval criterion is the surface of the stamped U-bend. Scratches on this surface cannot be accepted. On a four-level scale (starting with 0 and ending with 3), only levels 0 and 1 can be accepted. The tool concept that manages 50,000 U-bends (strokes) in the selected sheet material without class 2 surface is approved. This approval signifies that the tool concept is allowed to be used to make production tools for the selected sheet material. This is illustrated in Fig. 3.
- a tool to trim/blank/cut the sheet material grade of interest. This tool is set up in the same eccentric press as in the U-bend test above. The sheet material grade of interest is trimmed along a 150 mm long straight line in this tool. The approval criterion is the burr height on the trimmed/blanked/cut sheet. For approval, this burr height must be lower than 10% of the sheet thickness. A tool concept that manages 100,000 strokes with a burr height lower than 10% of the sheet thickness is approved.

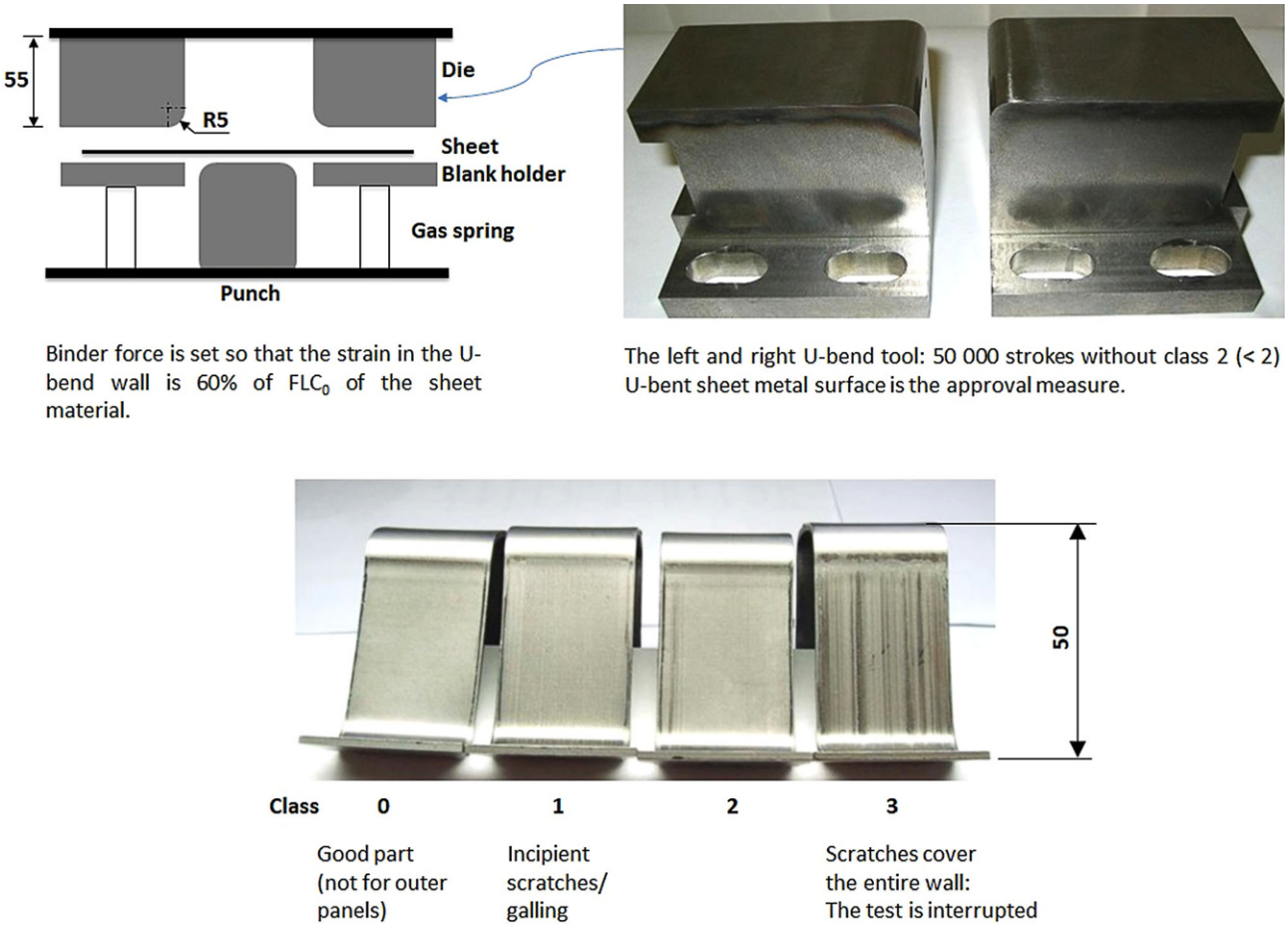

Fig. 3: The experimental set-up for certification of the forming (U-bending) tool. (See also [17])

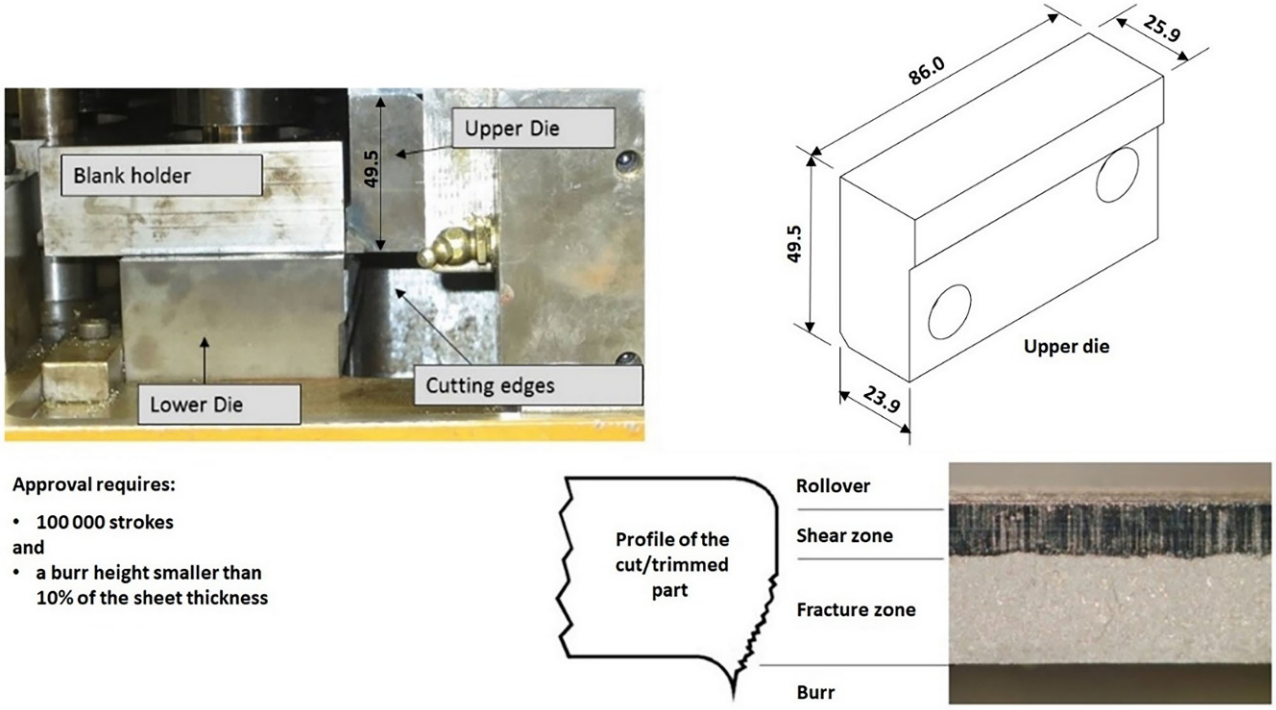

Fig. 4: The experimental set-up for certification of the trimming/blanking/cutting tool. The trimming is conducted by 2 upper dies mounted along a straight line. (See also [17])

The approval signifies that the tool concept is allowed to be used to make production tools for the selected sheet material. This is illustrated in Fig. 4.

For the certification in this study, the stamping tool concept comprises DIN 1.2709 (Table 2), 3D-printed both solidly and after topology optimization, hardened to 55 HRC, and machined to a surface roughness of 0.2 μm. The selected sheet material is 2-mm thick hot-dip galvanized DP600 (Table 4).

The puller and the punch shown in Fig. 5 constitute one of the working stations in the progressive die for stamping of the car body part C-Bow Lower. In a previous investigation [9], this work station was made both conventionally and with an AM inclusive process. The part, C-Bow Lower, is made in 1-mm thick hot-dip galvanized D600. The puller and the punch shown in Fig. 5 were 3D-printed in DIN 1.2709 (maraging steel) in this previous investigation [9]. To explore the industrial potential of AM in stamping tool applications, the punch shown in Fig. 5 was topology optimized and 3D-printed in this investigation.

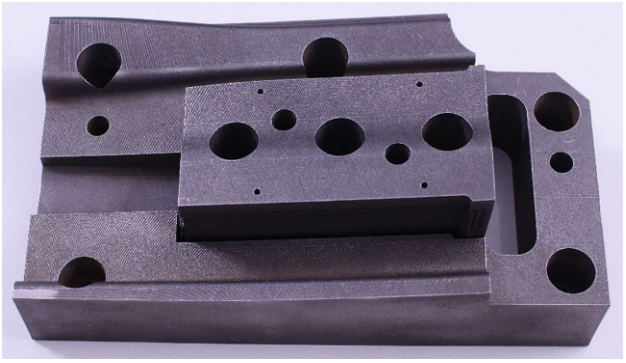

Fig. 5: The 3D-printed puller and punch in the progressive die. Material = DIN 1.2709. The inner structure is not solid. Both the puller and the punch are 3D-printed with a honeycomb inner structure (shown in Fig. 13). (See also [9])

All of the stamping tools in this study were 3D-printed in DIN 1.2709 with the process parameters shown in Table 7 and hardened by heat treatment at 490 °C in 6 h. The tools were 3D-printed and machined in collaboration with some of the project partner companies.

3.2 Injection Mold Core/Inserts

This study compares the cooling rates in an existing conventionally made injection molding core (tool inserts) with 3D-printed cores. The injection mold is designed to produce plastic (Polypropylene Homopolymer (PPH)) sofa clips (Fig. 6). The following two alternative core sets were developed, fabricated and compared with the conventionally made version:

- Alternative 1: The cooling channels were optimized by the toolmaker and the part producer based on these stake-holders' experiences in combination with the design freedom and flexibility provided by AM. This core set was made in DIN 1.2709 (Tables 2 and 7). After AM, the inserts were heat-treated at 490 °C in 6 h, after which they were cooled down in the furnace (in air).
- Alternative 2: Simulations were conducted to optimize the cooling channels in the core. The simulations are described in Sect. 4. Based on these simulations, the

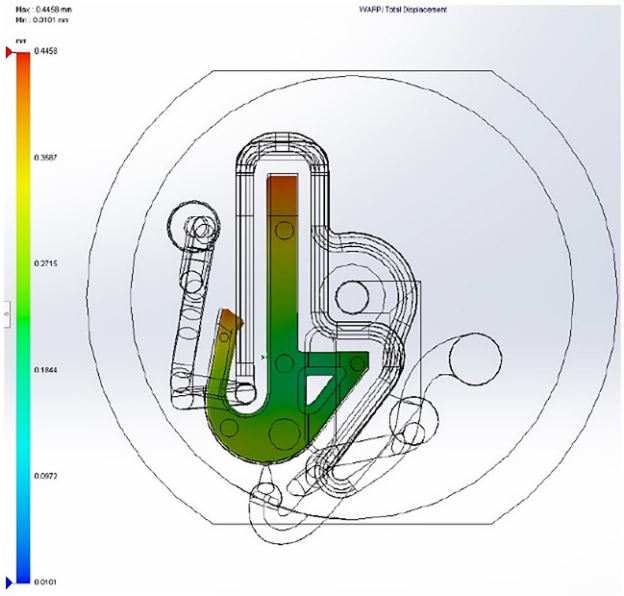

Fig. 6: This study focuses on the core (tool inserts) for injection molding of a plastic (Polypropylene Homopolymer (PPH)) sofa clip. Warpage (shape inaccuracy) of the sofa clip was minimized in the simulations

core parts were designed and 3D-printed in AM Corrax (Tables 6 and 7). After AM, the inserts were solution treated at 850 °C for 0.5 h (30 min) and aged at 525 °C in 4 h.

After hardening, these cores were machined to the right surface roughness. 0.5 mm was added to relevant surfaces of the 3D-printed cores for the subsequent post-machining. None of the inserts was coated. The inserts were 3D-printed and machined in collaboration with some of the partner companies (see Acknowledgments).

The optimized and 3D-printed cores were then compared in real production with the conventionally made version of the same core. During the production, the cooling was accomplished by injecting water through the cooling channels. In these tests, a cycle time reduction with a retained sofa clip gap size was the primary target. These production tests were conducted in the following fashion:

(i) The conventional core (inserts) was set up, and the part production was started. The cycle time was then measured and noted during the best conditions. The part dimensions and weight were measured and noted. Some parts were saved as examples.

(ii) The 3D-printed core (inserts) was set up and the part production was started. This 3D-printed core ran with the same settings as in step (i). If the part dimensions became the same as in step (i) or better, the cycle time was reduced. The reduced cycle time was noted. The part dimensions and weight were measured and noted. Some parts were saved as examples.

(iii) The results obtained in steps (i) and (ii) above were compared and evaluated.

4. Simulations—Topology, Cooling, and Cycle Optimization

4.1 Stamping Tools and Dies

LS-TaSC was used for the topology optimization of the U-bending tool. LS-TaSC is the tool for the topology optimization of non-linear problems analyzed by LS-DYNA involving time-varying loads and contact conditions.

In the topology optimization by LS-TaSC, a 3D model of the U-bending was created assuming that extrusion constraint prevailed. The cross-section of the design region is, in other words, assumed to be the same in the width direction, which makes the tool design insensitive for placement of the specimen in the width direction. To conduct the study, a symmetry model of the U-bend operation was created. The sheet specimen that is U-bent, 2-mm thick DP600 (Table 4), was modelled with MAT_133 (Barlat, YLD20000). During the loading, the displacements at the die profile radius were noted (see also [12, 13]).

The topology optimization of the (cutting/blanking/trimming) die in Fig. 4 is given in [14].

The industrial punch shown in Fig. 5 was first topology optimized using two different software packages (LS-Dyna/LS-TaSC and the AM Module in Siemens NX12.0) and subsequently 3D-printed in DIN 1.2709. (The work flow is best covered in the theory manual of each software package [15, 16]).

Fig. 7 displays the model created to topology optimize this punch using LS-TaSC. The design domain comprises the whole punch, except the cylinders around the three holes in the center of this punch. Nodes in the center of the holes are constrained in all directions. A pressure of 400 MPa is applied along the cutting edges (in an area that is 1 mm wide). Since the surface is inclined, the pressure will not act entirely in the z-direction. The magnitude of this pressure (400 MPa) is selected, since the punch is used to trim/cut 1-mm thick hot-dip galvanized DP600 (Table 4). The optimization objective was to maximize the stiffness

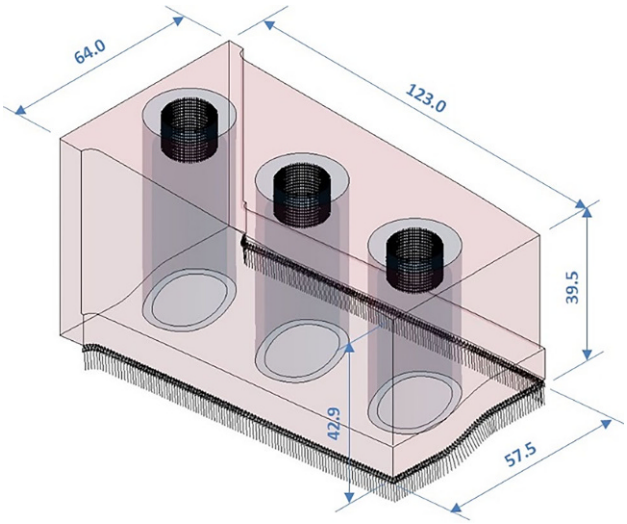

Fig. 7: The model for topology optimization of the industrial punch (Fig. 5) using LS-TaSC

at the mass fraction of 0.45, the reason for which will be accounted for in Sect. 5 (Results).

The model (Fig. 7) was also used to topology optimize the punch (Fig. 5) using Siemens NX12.0. The purpose of this "optimization" was to reduce the punch weight by 70% and to study the obtained punch shape and the maximum displacement at the cutting edge.

4.2 Injection Mold Core/Inserts

Using Solidworks Plastics, simulations were conducted to optimize the injection mold core (inserts) with respect to cooling and solidification of the molded part, the PPH sofa clip. Conformal cooling channels were designed based on solidification, cooling, heat flux, average mold temperature per cycle, average mold temperature at the end of the cycle, and warpage of the molded part. The inserts optimized by these simulations were 3D-printed in AM Corrax.

5. Results

5.1 Stamping Tools and Dies

Fig. 8 displays the results of the topology optimization of the U-bend tool (Fig. 3). Using LS-TaSC, the design domain was optimized at different mass (or volume) fractions (the figure above each tool). In Fig. 8, the fully red (and dark blue) indicates solid material, and white means no material. The objective (in the optimization) was to minimize the maximum internal energy density for the target mass fraction, i.e. to find a design with a uniform internal energy distribution [15]. A full process modelling approach was used, applying tool loads, displacements, and constraints on selected degrees of freedoms [12].

Three measures were used to evaluate the tools in Fig. 8:

- the mass fractions of the design region,
- the maximum von Mises stress in the design region during the complete simulation, and
- the vertical displacement time history of a node slightly above the draw radius.

Additionally, the thickness reduction in the formed U-bend wall was evaluated as a measure of how stretched it was during forming.

The maximum von Mises stress was 128 MPa in the solid tool and 205 MPa in the tool with the fraction of 0.45. The maximum thickness reduction in the wall of the formed U-bend was about 7.5% in both the solid tool and the tool with the fraction of 0.45.

Fig. 9 displays the maximum vertical displacement of a node at the die profile radius (during U-bending). The mass (or volume) fraction 0.45 gives, as shown in Fig. 9, the greatest material efficiency at a stiffness value very close to that of the fully solid (mass fraction 1). As mentioned above, the maximum von Mises stress and the thickness reduction with this fraction are also reasonable. Therefore, the fraction 0.45 was selected for the experimental study. For a more detailed description of the simulation results, the reader is referred to [12].

Fig. 10 displays the U-bending tool. The right tool half is 3D-printed as a fully solid piece. The left tool half is topology optimized at a mass fraction of 0.45 and 3D-printed. Both tool halves are 3D-printed in DIN 1.2709. The initial hardness was 56 HRC and the initial surface roughness was $R_a = 0.2\,\mu m$ in both cases. Both tool halves managed 50,000 strokes in 2-mm thick hot-dip galvanized DP600 with approved U-bend surfaces. Initially, the profile radius of the left tool half (topology optimized) was 5.05 mm and that of the right tool half (fully solid) was 5.04 mm. After 50,000 strokes, the maximum wear measured as a change in the profile radius was only 0.0186 mm.

Fig. 11 displays the 3D-printed solid and topology optimized trimming/blanking/cutting tool. Both versions are 3D-printed in DIN 1.2709. The hardness varies between 54 and 56 HRC and the surface roughness $R_a = 0.2\,\mu m$. Both tool versions managed 100,000 strokes in 2-mm thick hot-dip galvanized DP600 with a burr height lower than 0.2 mm and were thereby approved. After 100,000 strokes, the maximum wear measured as a change in the profile radius was 0.100 mm in the fully solid tool and 0.196 mm in the topology optimized tool.

Fig. 12 shows the shape and the resultant displacements before unloading in the industrial punch with the original solid design and the same punch topology optimized with

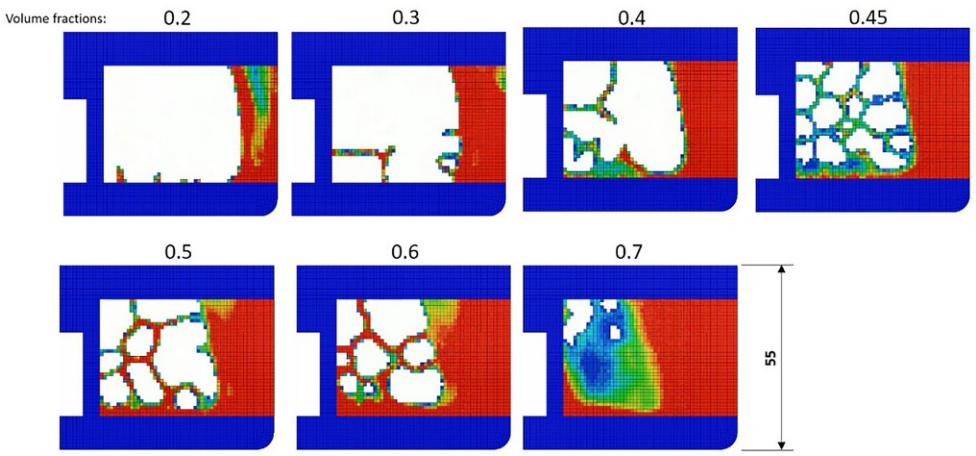

Fig. 8: Topology optimization of the U-bend tool with different volume fractions, i.e. the figure above each tool. In the design domain, *white*= no material, *blue*= almost no material, and *red*= solid (volume fraction = 1) [12]

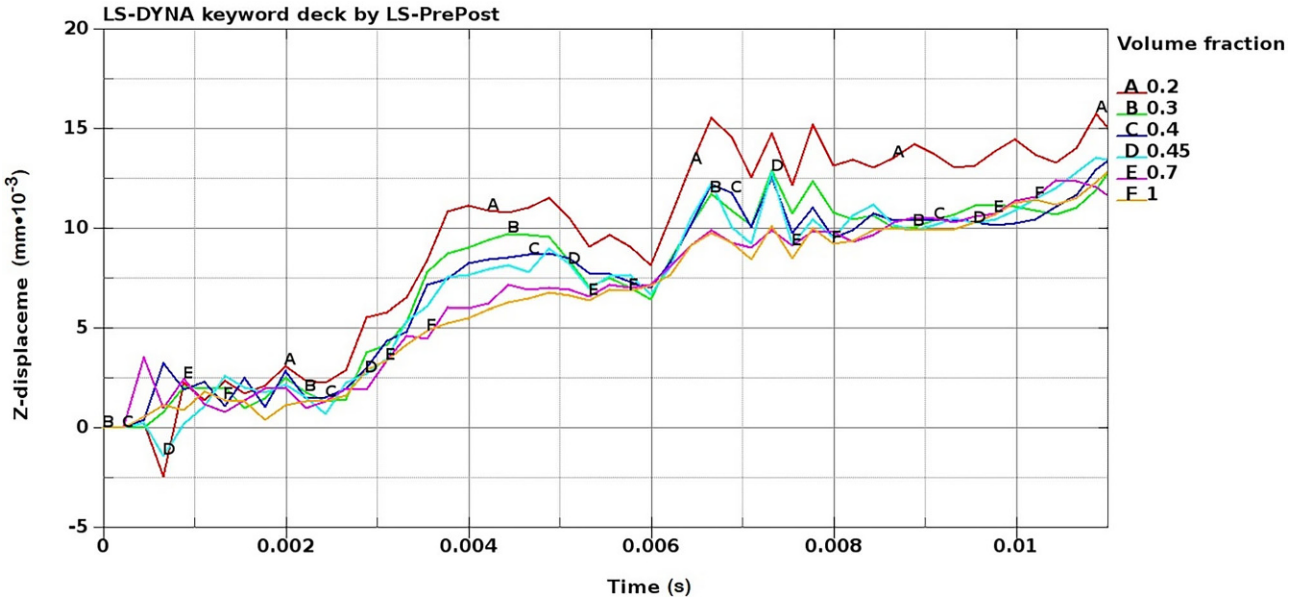

Fig. 9: The Z-displacement at the tool/die profile radius for different volume fractions [17]

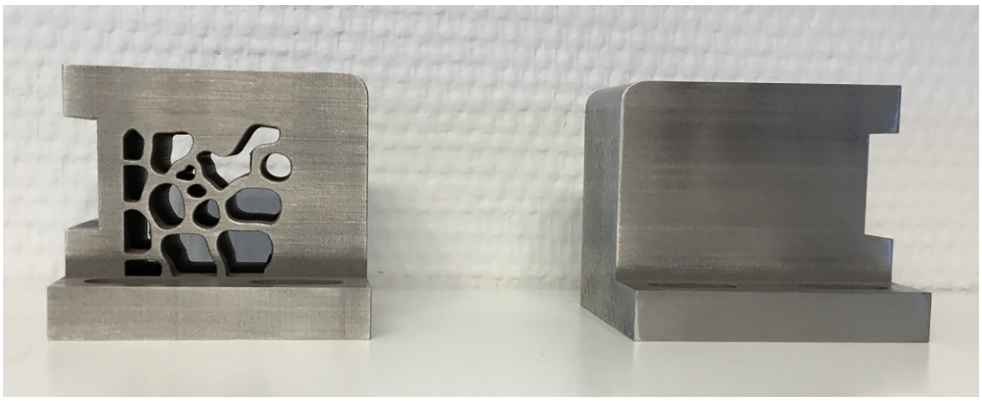

Fig. 10: The U-bending tool: the right tool half is 3D printed as a solid piece. The left tool half is topology optimized at a mass fraction of 0.45 and 3D printed. Both tool halves are 3D-printed in maraging steel DIN 1.2709. Both tool halves managed 50,000 strokes [9]

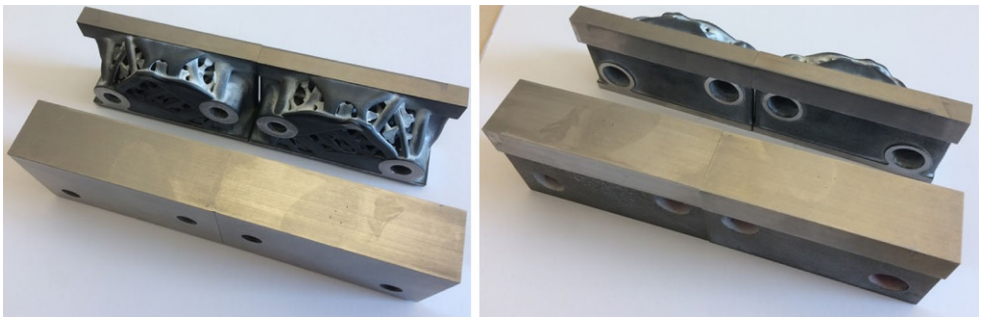

Fig. 11: 3D-printed solid and topology optimized trimming/blanking/cutting tool. Both versions are 3D-printed in DIN 1.2709. The hardness varies between 54 and 56 HRC. Both tool versions managed 100,000 strokes [17]

the volume/mass fraction of 0.45. This figure displays the results obtained with LS-TaSC in LS-DYNA. As mentioned previously, the punch is used to trim a sheet metal part made in 1-mm thick hot-dip galvanized DP600. The displacements in Fig. 12 arise due to this trimming.

The punch shown in Fig. 12b is topology-optimized using LS-TaSC with volume/mass fraction target of 0.45. This mass fraction was selected to give approximately the same weight reduction as the honeycomb inner structure.

Fig. 13 displays the 3D-printed topology optimized punch, and the 3D-printed (with honeycomb inner structure) conventionally designed version of the same punch. Compared to a 3D-printed solid punch, topology optimization and a honeycomb inner structure improved the material usage (and thereby reduced the weight) and printing time by ca 45% & ca 34% respectively. This means that the same printing time reduction and improved material efficiency can be accomplished in at least two different

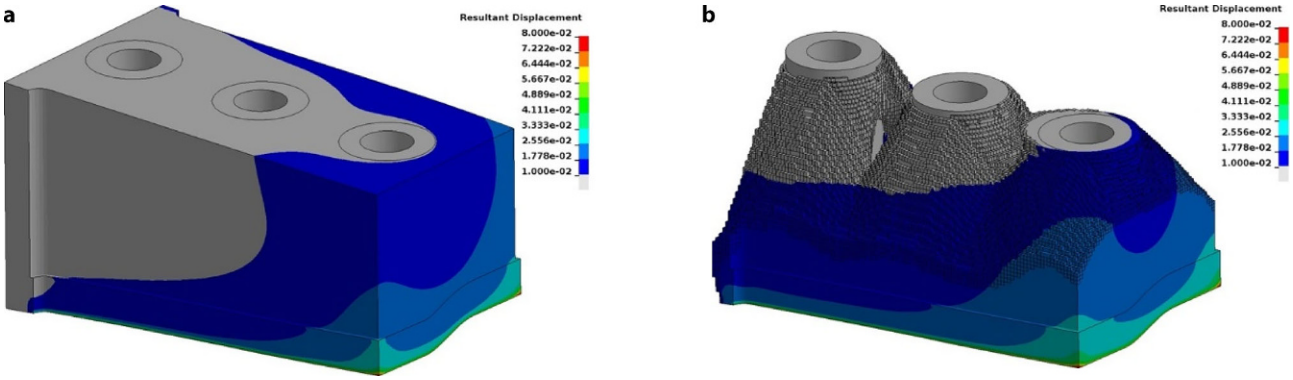

Fig. 12: The shape and the resultant displacements prior to unloading in the punch **a** with the original design and **b** topology optimized with the volume fraction 0.45 using LS-TaSC. In both cases, the punch is used to trim 1-mm thick hot-dip galvanized DP600 [17]

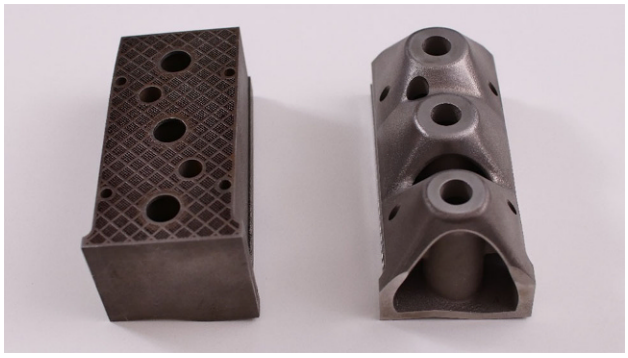

Fig. 13: The studied industrial punch (Fig. 5): Conventionally designed and 3D-printed with a honeycomb inner structure (*left*) and 3D-printed after topology optimization using LS-TaSC (*right*). Material = DIN 1.2709 in both cases [17]

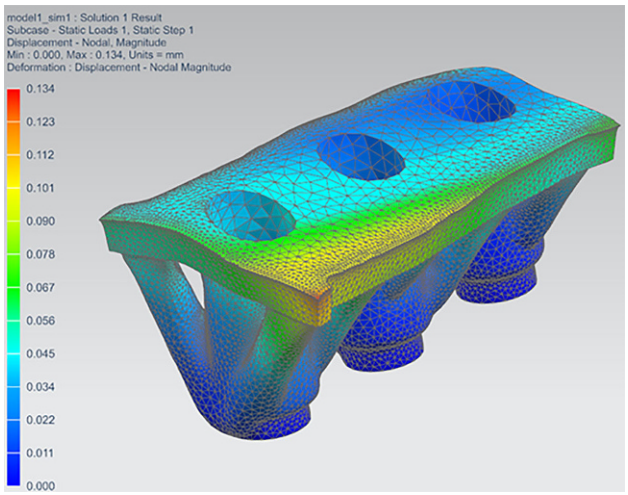

Fig. 14: The shape and the resultant displacements prior to unloading in the punch topology optimized using NX12 and targeting a weight reduction by 70% (compared to the conventionally designed solid version)

fashions—topology optimization and a honeycomb inner structure.

Fig. 14 shows the industrial punch topology-optimized using NX12 and targeting a weight reduction by 70% (compared to the solid version made conventionally). This figure depicts the shape after topology optimization and the resultant displacements (prior to unloading) in the trimming of 1-mm thick hot-dip galvanized DP600. The maximum displacement is, as shown in Fig. 14, much larger than those in Fig. 12b. This much larger displacement is held to have a large negative impact on the trimming result (the rollover, shear zone length, fracture zone length, and burr height in Fig. 4) and the die life length. Since the NX12 topology is similar to the LS-TaSC solution, much of the differences are believed to be explained by the larger targeted weight reduction in the NX12 solution.

Fig. 15: The studied industrial punch (Fig. 5): 3D-printed after topology optimization using NX12 (Fig. 14). Material = DIN 1.2709

The industrial punch topology-optimized using NX12, was 3D-printed in DIN 1.2709, Fig. 15.

5.2 Injection Mold Core/Inserts

As mentioned in Sect. 3.2, two (2) different design and material alternatives were developed and tested in this investigation.

Alternative 1: The core/inserts for injection molding of the plastic (PPH) sofa clip optimized in accordance with the toolmaker's and part producer's experiences in combination with the design freedom and flexibility provided by AM. After design optimization based on the toolmaker's and part producer's preferences, this core set was 3D-printed in DIN 1.2709. After hardening and post-treatment, this core has a hardness of 55 HRC and a surface roughness $R_a = 0.2\,\mu m$.

Alternative 2: Simulations were conducted, using Solidworks Plastics to optimize the core/inserts for injection molding of the plastic (PPH) sofa clip. This simulation-based optimization resulted in the core/inserts depicted in Fig. 16. The core/inserts obtained by the simulation-based cooling channel optimization (Fig. 16) was 3D-printed in Uddeholm AM Corrax. Fig. 17 displays these inserts, which were hardened to 48 HRC and post-machined to the surface roughness $R_a = 0.2\,\mu m$.

The optimized and 3D-printed inserts were tested in real production and compared with the existing conventionally designed and manufactured core in accordance with the procedure described in Sect. 3.2. This comparison showed that

- the water flow was reduced by
  - 50.6% in the core optimized in accordance with the preferences of the toolmaker and part producer and 3D-printed in DIN 1.2709.
  - 86.4% in the core optimized by simulations and 3D-printed in Uddeholm AM Corrax, Figs. 16 and 17.
- the cycle time could be reduced somewhat with the core/inserts 3D-printed in Uddeholm AM Corrax (Figs. 16 and 17).

5.3 Weights, Costs, and Lead Times

The weights, costs, and lead times for the tools, dies, and molds (core/inserts) in this investigation are summarized in Table 8. This table comprises both the tools, dies, and molds that were made conventionally (existing tools) and

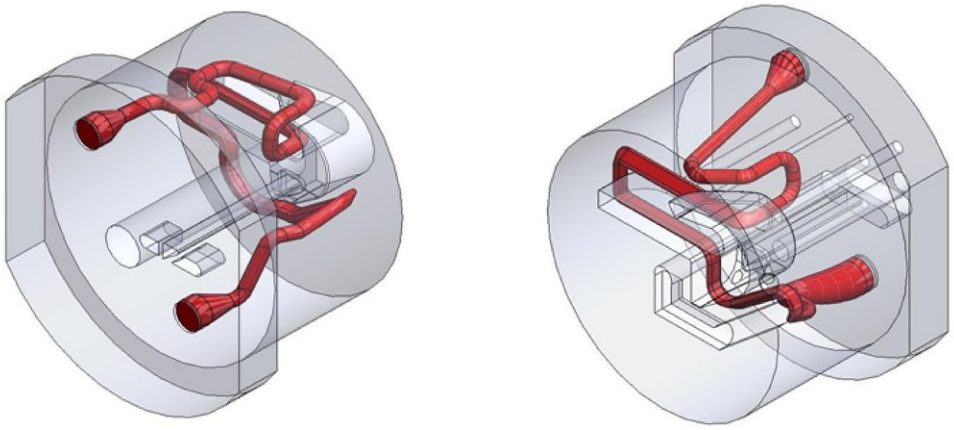

Fig. 16: The core/inserts for injection molding of the sofa clip optimized by the simulations. *Red* color = the cooling channels after optimization

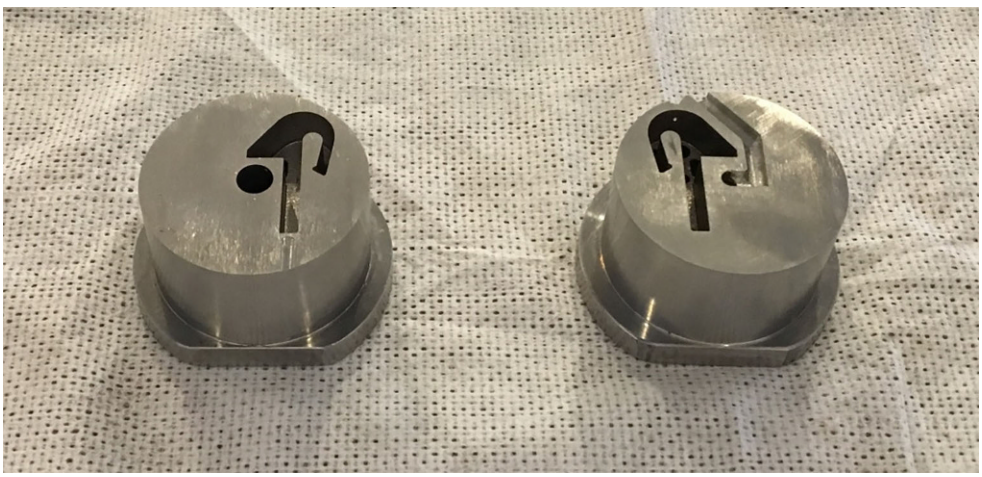

Fig. 17: The core/inserts for injection molding of the sofa clip cooling channel optimized by simulations (Fig. 16) and 3D-printed in Uddeholm AM Corrax [13]

TABLE 8
The tools, dies and molds made in this study: weights, lead times and costs (SEK = Swedish Crowns/Kronor)

Tool	Variant	Weight[a] (g)	Lead time (days[b])	Cost (SEK) DEPR[c] = 6 yrs	Cost (SEK) DEPR[c] = 15 yrs
Trimming/ cutting/ blanking tool	Conventional, solid	815	12	7,500	7,500
	3D-printed, solid	812	3.3	17,010	7,490
	3D-printed, topology optimized	428	3.17	13,345	7,365
U-bend tool	Conventional, solid tool half	1137	12	10,000	10,000
	3D-printed, solid tool half	1137	3.25	25,138	12,113
	3D-printed, topology optimized tool half	916	3.25	23,412	11,412
Punch	Conventional, solid	2510	8	10,500	10,500
	3D-printed, honeycomb inner structure	1360	3.7	34,825	16,600
	3D-printed, topology optimized, LS-TaSC	1400	3.7	34,825	16,600
	3D-printed, "topology optimized", NX12	764	3.1	19,900	10,640
Injection molding core (inserts)	Conventional	1042	14	20,000	20,000
	3D-printed in DIN 1.2709	1055	3.5	34,355	21,200
	3D-printated in Uddeholm AM Corrax	1082	3.5	Contact Uddeholm	

[a]Weight of the fully processed tool
[b]Each day = 24 h
[c]DEPR = the depreciation time/period for the 3D-printing/AM machine

those made with an AM inclusive process (these were made in this investigation).

For the stamping tools and dies in this study, an AM inclusive process consists of 3D-printing, cleaning, heat treatment, and machining. For the injection molding core/inserts in this study, an AM inclusive process consists of 3D-printing, cleaning, EDM (electrical discharge machining), heat treatment, and machining (Table 8).

The weight value in Table 8 is the weight of the fully processed tool, i.e. the ready-made 3D-printed and post-processed tool or the ready-made conventionally manufactured tool.

The values in Table 8 are evaluated and approved by the partners and reflect the industrial infrastructure in this project. The lead times and costs displayed in Table 8 are estimated to have been ca 8–10% lower if all of the toolmaking operations could have been conducted in-house at an Original Equipment Manufacturer (OEM).

The lead time for each tool variant in Table 8 comprises the time it took from "order to delivery", i.e. the time it took to carry out manufacturing engineering, manufacturing (i.e. 3D-printing and post-processing in an AM inclusive process) and all transportations.

The cost of each tool variant in Table 8 comprises all costs from "order to delivery", i.e. the costs of material, labor, machines, working space, gas, energy, media, consumables, maintenance, transportation, and overheads.

The length of the depreciation period/time for the 3D-printing/AM machine plays a significant role. A 15-year long depreciation period yields lower costs. Yet, such a long period might not be acceptable, since the technology is still young and the machines launched 6 years from now will most probably be much more sophisticated than the current.

As displayed in Table 8, 3D-printing results in a significantly improved material efficiency and reduced lead time. The total cost of each tool variant made by an AM inclusive process is, however, in all cases higher than the corresponding conventionally made tool if the depreciation period for the 3D-printing machine is 6 years long. This higher total cost might be acceptable for stamping tools and dies, especially for late changes. For the injection molding core (inserts), the costs of the 3D-printed variants are higher than that of the conventionally fabricated core. Yet, the total cost per produced unit/part is estimated to be lower, since the 3D-printed tool variant results in a somewhat shorter cycle time. A cycle time reduction leads generally to lower total annual costs. The results and evaluations made in this study show, in other words, that

- it is not possible to verify Fig. 1 as far as tool manufacturing—low volume production—is concerned. 3D-printing/AM results in higher costs than conventional manufacturing in low volume production (tool making in this investigation).
- Fig. 2 can be considered as verified for injection molding core/inserts. 3D-printing/AM results in higher core costs (larger initial investment) but the total cost per produced part can be reduced due to improved cooling and shorter cycle time.

Based on the results in this study, the authors tend to agree with the high manufacturing readiness level for AM of production tools.

6. Conclusions

The following conclusions can be drawn:

- *Stamping tools and dies for 1-mm and 2-mm thick hot dip galvanized DP600*: 3D-printed DIN 1.2709 is approved as a tool concept. Both conventional and topology optimized stamping tools & dies yield approved results. The same printing time reduction and improved material efficiency can be accomplished by either topology optimization or a honeycomb inner structure.
- *Injection molds*: The cooling and cycle time can be improved with an optimized core (inserts) 3D-printed in Uddeholm AM Corrax. The best results are obtained if the 3D-printed core is not only an optimized copy of the conventionally designed and manufactured version. The best results are obtained if the core is redesigned to utilize the full potential of 3D printing. 3D-printing/AM results in higher core costs (larger initial investment) but the total cost per produced part can be reduced due to improved cooling and shorter cycle time.
- *Stamping tools and dies and injection molds*: 3D-printing improves the material usage and lead time significantly. The depreciation period for the 3D-printing/AM machine plays a significant role, as far as the tool costs are concerned. 3D-printing/AM results in higher costs than conventional manufacturing in low volume production, i.e. tool making in this investigation.

Acknowledgements. The authors would like to thank Sweden's Innovation Agency Vinnova for funding this investigation and 3D MetPrint, Dynamore Nordic, Hydroforming Design Light, IKEA, Ionbond Sweden, Melament, Nolato Lövepac, PLM Group, RISE IVF, Volvo Cars, Uddeholm and Örebro University for a fruitful and efficient collaboration.

This paper was selected by ASMET for publication in BHM.

Funding. Open access funding provided by Örebro University.

References

1. Ålgårdh, J.; Strondl, A.; Karlsson, S.; Farre, S.; et al.: State-of-the-Art for Additive Manufacturing of Metals. Report 2016-03898—State-of-the-art—Version 2.1, Swedish Arena for Additive Manufacturing of Metals, 22 June 2017, 2017
2. Additive Manufacturing, Chapter 6—Technology Assessment, Quadrennial Technology Review 2015, US Department of Energy, 2015.
3. Ålgårdh, J.; Strondl, A.; Karlsson, S.; Farre, S.; et al.: Research Needs and Challenges for Swedish Industrial Use of Additive Manufacturing, RAMP-UP, Report 2016-03898—Research Needs and Challenges—Version 2, Swedish Arena for Additive Manufacturing of Metals, 6 October 2017, 2017
4. Mueller, B.; Hund, R.; Malek, R.; Gebauer, M.; et al.: Added Value in Tooling for Sheet Metal Forming through Additive Manufacturing. Proceedings of the International Conference on Competitive Manufacturing, COMA '13, 30 January–1 February 2013, Stellenbosch, South Africa 2013
5. Leal, R.; Barreiros, F. M.; Alves, L.F.; Romeiro, F.; et al.: Additivee manufacturing tooling for the automotive industry, Int J Adv Manuf Technol, 92 (2017), pp 1671–1676
6. Shinde, M. S.; Ashtankar, K. M.: Additivee manufacturing–assisted conformal cooling channels in mold manufacturing processes, *Advances in Mechanical Engineering*, 9 (2017), no. 5, pp 1–14
7. Shellabear, M.; Weilhammer, J.: Tooling applications with EOSINT M, Whitepaper, Electro Optical Systems, EOS GmbH, München, Germany, 2007
8. Additive manufacturing—a game-changer for the manufacturing industry? Roland Berger Strategy Consultants, November 2013, Munich, Germany, 2013
9. Asnafi, N.; Shams, T.; Aspenberg, D.; Öberg, C.: 3D Metal Printing from an Industrial Perspective—Product Design, Production and Business Models, BHM Berg- und Hüttenmännische Monatshefte, 164 (2019), no. 3, pp 91–100
10. According to 3D System's website https://www.3dsystems.com/ (July 6, 2018)
11. According to Tunnplåtskatalogen (The sheet metal catalogue in Swedish), Tibnor, March 2009, downloaded from http://www.tibnor.se on July 6, 2018
12. Aspenberg, D.; Asnafi, N.: Topologyy optimization of a U-bend tool using LS-TaSC. Proceedings of the 12th European LS-DYNA Conference, 14–16 May, 2019, Koblenz, Germany, 2019
13. Asnafi, N.; Alveflo, A.: 3D Metal printing of Stamping Tools & Dies and Injection Molds. Proceedings of at Tooling 2019 Conference and Exhibition, 12–16 May, 2019, Aachen, Germany, 2019
14. Strömberg, N.: Design Optimization by using Support Vector Machines. Proceedings of NAFEMS NORDIC Conference 18, 24–25 April, 2018, Göteborg, Sweden, 2018
15. Livermore Software Technology Corporation, The LS-TaSC™ Tool—Theory manual, Version 4, 2018
16. Wills, G.: NX12 Topology Optimization for Designers, Siemens PLM Software, Siemens AG, 2017
17. Asnafi, N.; Rajalampi, J.; Aspenberg, D.: Design and Validation of 3D-Printed Tools for Stamping of DP600, 2019 IOP Conf. Ser.: Mater. Sci. Eng., 651 (2019), p 012010